JMEPEG (2004) 13:530-536
DOI: 10.1361/10599490420601

1059-9495/$19.00

Dry and Clean Age Hardening of Aluminum Alloys by High-Pressure Gas Quenching

A. Irretier, O. Kessler, F. Hoffmann, and P. Mayr

(Submitted December 10, 2003)

When precipitation-hardenable aluminum parts are water quenched, distortion occurs due to thermal stresses. Thereby, a costly reworking is necessary, and for this reason polymer quenchants are often used to reduce distortion, with the disadvantage that the quenched parts have to be cleaned after quenching. In opposition to liquid quenchants, gas quenching may decrease distortion due to the better temperature uniformity during quenching. Furthermore, cleaning of the quenched parts can be avoided because it is a dry process. For this purpose, a heat-treating process was evaluated that included a high-pressure gas-quenching step. Gas quenching was applied to different aluminum alloys (i.e., 2024, 6013, 7075, and A357.0), and tensile tests have been carried out to determine the mechanical properties after solution annealing, gas quenching, and aging. Besides high-pressure gas quenching, alloy 2024 was quenched at ambient pressure in a gas nozzle field. The high velocity at the gas outlet leads to an accelerated cooling of the aluminum alloy in this case. Aluminum castings and forgings can be classified as an interesting field of application of these quenching methods due to their near-net shape before the heat treatment. Cost savings would be possible due to the reduced distortion, and therefore, less reworking after the precipitation hardening.

Keywords aluminum, distortion, gas quenching, mechanical properties, precipitation hardening

1. Introduction

Precipitation hardening of aluminum alloys requires high quenching rates after solution annealing to avoid coarse intermetallic precipitates at the grain boundaries. A supersaturated solution of the alloying elements is a requirement for the formation of fine intermetallic precipitates during aging, which improve the mechanical properties. Water is used predominantly nowadays to suppress coarse precipitates during quenching. Due to the Leidenfrost phenomenon, distortion occurs as a result of the formation and collapse of a vapor blanket around the part.[1] This nonuniform cooling causes distortion, especially in thin or complex-shaped parts (e.g., sheets, castings, or forgings), and makes costly reworking necessary.[2] The control of the cooling rate is only possible by varying the temperature of the water or by adding additives like polymers to the aqueous quenching medium. Furthermore, where polymers have been used for the control of the quenching process, it is necessary to clean the parts.

During the high-pressure gas quenching, parts are immersed in a cooling gas instead of an aqueous medium. Because the Leidenfrost phenomenon is absent, the improved temperature uniformity provides an opportunity to manufacture parts with only slight distortion, and this can reduce the costs related to reworking or excess scrap. By varying the gas pressure, gas velocity, or the gas itself, a well-directed manipulation of the cooling rate is possible.[3]

A. Irretier, O. Kessler, F. Hoffmann, and **P. Mayr,** Foundation Institute for Material Science, Bremen, Germany. Contact e-mail: irretier@iwt-bremen.de.

Besides gas quenching under high pressure in a cooling chamber, cooling is also possible at ambient pressure in a gas nozzle field. In this case, the flow velocity and degree of turbulence can be increased and varied by the primary pressure, the shape of the nozzles, or the number and arrangement of the nozzles.[3,4]

Age-hardenable aluminum alloys are often quench-sensitive, on the one hand, requiring a high cooling rate to create the desired microstructure and the mechanical properties, while on the other hand, requiring a cooling rate as slow as possible to reduce the distortion and residual stresses in the part. In consideration of both requirements, the potential to reduce distortion exists by using high-pressure gas quenching or nozzle field quenching. For both possibilities, the following question arises: is the cooling rate during quenching sufficient to obtain the specific required strength after aging of the aluminum alloys? Therefore, the primary aim of this work was to prove that high-pressure gas quenching and nozzle field quenching are reliable processes for the precipitation hardening of aluminum alloys with high quench sensitivity.

2. Quench Factor Analysis

Quench factor analysis (QFA) is a procedure that is used to correlate the quench rate in a part with the precipitation behavior during the quenching process.[5] To understand the precipitation behavior, one must recognize that the rate of precipitation during quenching depends on two competing factors: supersaturation and diffusion. At high temperatures, supersaturation is low, and so the precipitation rate is low despite the high diffusion rate. At low temperatures, the diffusion rate is low, and thus the precipitation rate is low despite the high degree of supersaturation. At intermediate temperatures, the precipitation rate is highest. Consequently, the times needed to produce equal amounts of precipitation at a given temperature

Table 1 Constants for calculating *C*-curve and quench factor at 99.5% of attainable yield strength[7]

Alloy	K_1 [–]	K_2, s	K_3, J/mol	K_4, K	K_5, J/mol
7075-T73	0.00501	1.37×10^{-13}	1069	737	1.37×10^5

(i.e., isothermal conditions) follow a C-shape pattern. For these C-curves, Eq 1 was developed.[5,6]

$$C_T = K_1 * K_2 * \exp\left(\frac{K_3 * K_4^2}{R * T(K_4 - T)^2}\right) * \exp\left(\frac{K_5}{R * T}\right) \quad \text{(Eq 1)}$$

where C_T is the critical time required to precipitate a constant amount, K_1 is a constant that equals the negative natural logarithm of the fraction not precipitated, K_2 is a constant related to the reciprocal of the number of the nucleation sites, K_3 is a constant related to the energy required to form a nucleus, K_4 is a constant related to the solvus temperature, K_5 is a constant related to the activation energy for diffusion, R is the gas constant (8.3143 J/Kmol), and T is the temperature (K).

If the numerical values for the constants in Eq 1 are known, the C-curve for each particular alloy can be constructed. Typical K values for alloy 7075-T73 are given in Table 1.[7] In the underlying investigation, alloy 7075 was solution heat treated at 460-471 °C, quenched, and aged at 100-112 °C for 6-8 h and at 170-182 °C for 8-10 h.

Using the K values from Table 1 in Eq 1, the calculation of the C-curve for 7075-T73 is possible, as is shown in Fig. 1. After recording the cooling curves, these continuous cooling curves can be compared with the isothermal C-curves by QFA. For this purpose, the cooling curves have to be split into isothermal steps (Δt) at certain T values. The C_T value is then calculated at these temperatures using Eq 1. The ratio of the time step length, Δt, divided by the C_T value provides the incremental quench factor (q), which is calculated using Eq 2.[5]

$$q = \frac{\Delta t}{C_T} \quad \text{(Eq 2)}$$

The sum of the incremental quench factors during cooling of the parts through the critical temperature range, normally defined as being between 425 and 150 °C, results in the quench factor Q corresponding to Eq 3.[5]

$$Q = \sum_{150}^{425} q = \sum_{150}^{425} \frac{\Delta t}{C_T} \quad \text{(Eq 3)}$$

High quench rates are associated with low Q values, minimum precipitation during quenching, and therefore, high yield strengths after aging. Conversely, higher Q values indicate slower quench rates and lower strength values. The prediction of the attainable yield strength from a given cooling curve is then possible using Eq 4.[5]

$$\sigma_Y = \sigma_{max} e^{-K_1 Q} \quad \text{(Eq 4)}$$

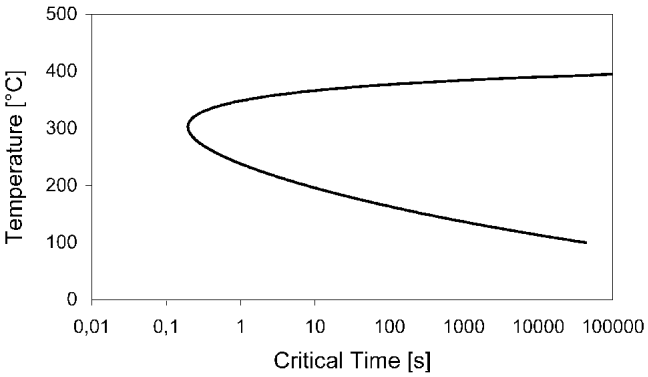

Fig. 1 Calculated C_T-curve (AW-7075-T73)

where σ_Y is the predicted yield strength, and σ_{max} is the yield strength after an infinite quench and following temper cycle.

3. Experimental Procedure

The required cooling rate strongly depends on the chemical composition of the aluminum alloy. Particular attention in this work was given to quench-sensitive aluminum alloys, in which, in fact, a water or polymer quench seems to be needed to obtain a supersaturated solution. In consequence of the Leidenfrost phenomenon, which promotes the distortion, these quench-sensitive alloys are, therefore, simultaneously vulnerable to distortion. Corresponding to Table 2, three different aluminum wrought alloys and one cast alloy have been used for the investigations.

The solution annealing as well as the aging of the alloys was equal to the conventional heat treatment with water quenching. Temperatures and times match the normal values used for precipitation hardening of the alloys.[8,9]

3.1 High-Pressure Gas Quenching

Corresponding to Table 3, wrought alloys 2024 and 7075 were available as plates, 20 mm in thickness, while alloy 6013 was available as plates, 4.5 mm in thickness. The cast alloy A357.0 was already available as cylindrical tensile specimens with a length of 120 mm and a diameter of 8 mm. These samples were made by investment casting.

By varying the specimen thickness of the wrought alloys between 3 and 20 mm, a decreasing cooling rate with an increasing specimen thickness could be achieved. In this manner, it was possible to correlate the measured strength of the specimens with the different cooling rates during high-pressure gas quenching. After gas quenching and aging, three flat tensile specimens were manufactured from each quenching sample thickness corresponding to DIN 50125-Form E. Flat tensile specimens with a thickness of 3 mm were taken from the core of the 20 mm thick quenched plates. In the case of the casting alloy A357.0, five specimens (Form B) have been used for the determination of the mechanical properties.

Solution annealing and high-pressure gas quenching were realized in a double-chamber vacuum furnace type IPSEN In-

Table 2 Investigated aluminum alloys and their heat-treating parameters

Alloy	Solution annealing	Aging
AW-2024		
AlCu4Mg1	495 °C/70 min	RT/>96 h
AW-7075		
AlZn5,5MgCu	470 °C/70 min	120 °C/12 h +180 °C/11 h
AW-6013		
AlMg1Si0,8CuMn	565 °C/30 min	190 °C/4 h
A357.0		
AlSi7Mg 0.6	540 °C/825 min	160 °C/4 h

Table 3 Dimensions and shape of the specimen

Alloy	Quenching specimen	Tensile specimen DIN 50125
AW-2024 (20 mm)	160 × 30 × 3 mm	Form E/3 mm
	160 × 36 × 4 mm	Form E/4 mm
	210 × 60 × 6 mm	Form E/6 mm
	275 × 75 × 10 mm	Form E/10 mm
	160 × 100 × 20 mm	Form E/3 mm (core)
AW-6013 (4.5 mm)	160 × 30 × 3 mm	Form E/3 mm
	160 × 36 × 4 mm	Form E/4 mm
AW-7075 (20 mm)	160 × 30 × 3 mm	Form E/3 mm
	160 × 36 × 4 mm	Form E/4 mm
	210 × 60 × 6 mm	Form E/6 mm
	275 × 75 × 10 mm	Form E/10 mm
	160 × 100 × 20 mm	Form E/3 mm (core)
A357.0 (Ø8 mm)	120 × Ø8 mm	Form B/8 mm

ternational GmbH, Clive, Germany, RVTC 550 × 550 × 310 mm (Fig. 2).[10] The system is equipped with a heating chamber on the left side and a separated "cold" cooling chamber on the right side. Compared with single-chamber systems, higher cooling rates are possible because quenching takes place in a chamber with ambient temperature. Thus, it is not necessary to cool the chamber together with the batch. After solution annealing, the door between the chambers is opened, and the batch is transported into the cold chamber. The chamber is filled with the cooling gas, and the gas is continuously recirculated through the chamber. The quench delay can be neglected because solution annealing and transport have taken place in vacuum with only a minimal temperature loss to the specimens. For later applications, solution annealing and transport of the specimens will take place in atmosphere. In this case, the construction of the double-chamber furnace will be considerably easier, but it will still be possible to meet the required quench delay time to avoid the precipitation of the alloying elements during the transport.

For the temperature measurement in the core of the specimens (thickness between 3 and 20 mm), each batch setup was equipped with thermocouples. The specimens were mounted vertically on a batch holder to provide a large surface for the heat exchange between the specimens and the quenching gas. To obtain high quench intensities, helium was used as cooling gas at a pressure of 16 bar. The aging of the specimens was carried out in a conventional air furnace.

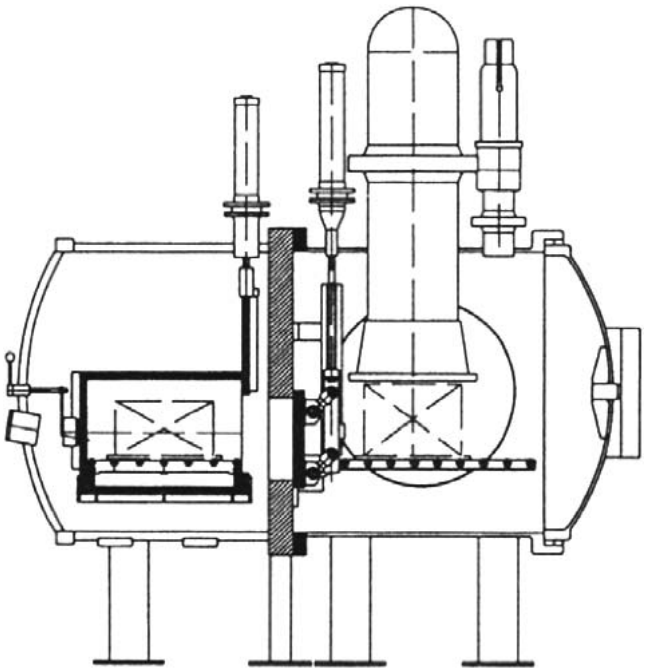

Fig. 2 Schematic of a double-chamber vacuum furnace[10]

3.2 Nozzle Field Quenching

Investigations on a gas nozzle field at ambient pressure have been carried out with tensile specimens (AW-2024) of different circular cross sections (Ø5, 8, and 12 mm) corresponding to DIN 50125-Form B.

As demonstrated in the experimental setup in Fig. 3, quenching took place in a nozzle field with four nozzle rows. Utilizing measurements with a hot wire anemometer, a gas (nitrogen) velocity of approximately 150 m/s was calculated at the gas outlet.

Solution annealing was carried out in a tube furnace, which was positioned above the nozzle field, using the heat-treating parameters for the alloy 2024, as listed in Table 2. After solution annealing, the specimens were dropped into the nozzle field. During quenching with nitrogen at ambient pressure, the temperature was measured in the core of reference specimens (Ø5, 8, and 12 mm). After quenching and aging, the tensile properties of the specimens were determined.

4. Results and Discussion

4.1 High-Pressure Gas Quenching

Regarding the precipitation of intermetallic phases during quenching, the temperature between 425 and 150 °C was defined as a critical interval for the QFA. Therefore, the cooling rate must be very high in this interval. From the cooling curves in Fig. 4, an average cooling rate of approximately 70 K/s was determined for a material thickness of 3 mm. The cooling rates decreased to 36 K/s for a thickness of 6 mm, 23 K/s for a thickness of 10 mm, and 10 K/s for a material thickness of 20 mm.

After aging, the mechanical properties of the specimens

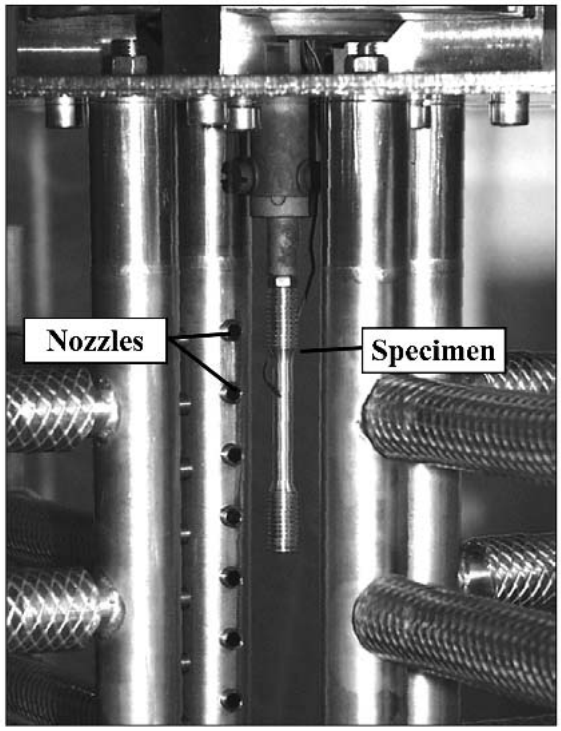

Fig. 3 Nozzle field with four nozzle rows and a tensile specimen in the center (alloy AW-2024; Ø5 mm)

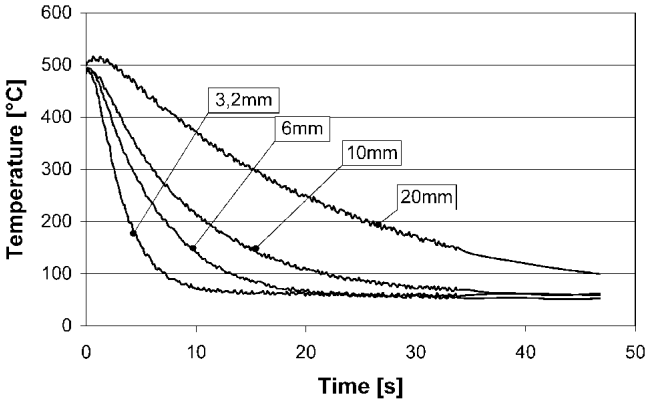

Fig. 4 Cooling curves with different specimen thickness (high-pressure gas quenching; He 16 bar; alloy AW-2024)

were determined in tensile tests. The results have been compared with the minimum required values for the relevant alloy standards. Furthermore, a conventional heat treatment with water quenching has been carried out for the direct comparison between water and gas quenching.

The mechanical properties of 6013-T6 are pictured in Fig. 5. After the conventional heat treatment with water quenching, as well as after the heat treatment with gas quenching, the mechanical properties exceed the minimum values[11] for a material thickness of 3 mm, whereby the values after water and gas quenching are nearly similar. The tensile properties of 2024-T4

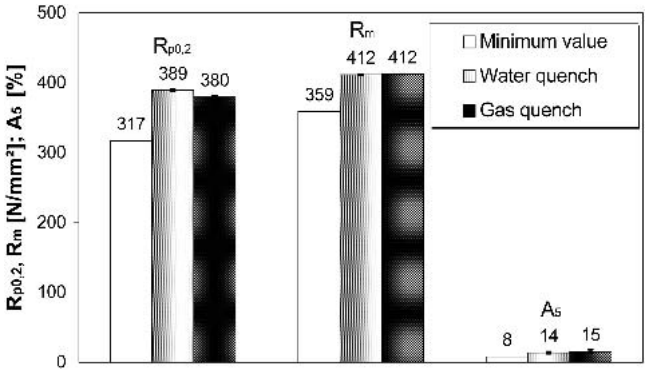

Fig. 5 Tensile properties of alloy AW-6013-T6 by comparison (3 mm, after aging at 190 °C for 4 h)

are shown in a scatter band with little variation around the minimum mechanical properties[12] for 2024-T4 up to a thickness of 20 mm (Fig. 6).

The tensile properties of 7075-T73 after gas quenching are compared in Fig. 7. Because this alloy is more quench sensitive than 2024-T4 under the same quench conditions, there is a greater loss in strength, and the minimum tensile properties[12] can be attained only up to a specimen thickness of approximately 5 mm. At this point, it has to be mentioned that the minimum tensile properties for 7075 in Fig. 7 are only valid in the heat-treating condition T7351 (i.e., stretched and overaged). The cold deformation during stretching leads to an increase in dislocation density and, therefore, to an increase in $R_{p0.2}$ and R_m. Therefore, the tensile properties should increase when an additional stretching is applied to the gas-quenched specimens before aging.

As already mentioned, a prediction of the yield strength is possible where the C-curve and the cooling curves are known. Both requirements are fulfilled for the alloy 7075-T73. Using Eq 1-4, it is possible to calculate the quench factor Q and the predicted yield strength σ_Y from the measured cooling curves at different specimen thicknesses during high-pressure gas quenching of the alloy.

The predicted yield strength in Table 4 was calculated from Eq 4 with a value of 450 MPa for the yield strength σ_{max}, because this was the maximum attainable yield strength after cold water quenching and aging of a thin section of the alloy 7075-T73. The measured yield strengths for the different specimen thicknesses are compared with the predicted yield strength curve σ_Y in Fig. 8. The measured yield strength is situated slightly below the predicted yield strength. The different aging conditions in this work and in the literature[7] are probably responsible for the lower measured values.

The yield strength after two-step aging is not only a function of the average quench rate, but also depends on the first-step aging temperature. Larger differences in yield strength were obtained with average quench rates below about 50 K/s.[13] Cooling rates between 10 and 50 K/s also have been measured during high-pressure gas quenching. The higher first-step aging temperature after gas quenching (120 °C), compared with the first-step aging temperature (100-112 °C) given in the literature,[7] would lead to lower yield strengths after the complete aging treatment. These uncertainties in QFA could be over-

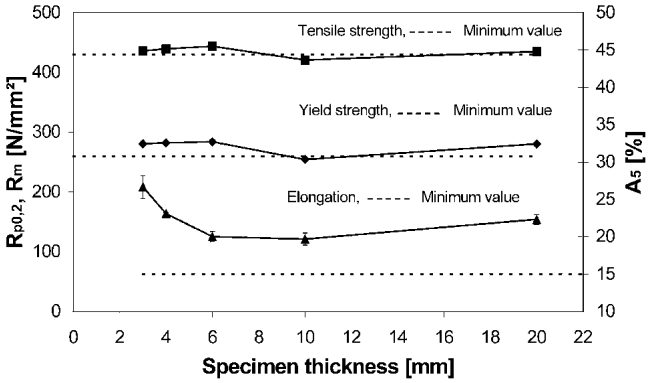

Fig. 6 Strength properties with increasing specimen thickness. Dotted line = minimum values (alloy AW-2024-T4, gas quench 16 bar aged at RT for >96h)

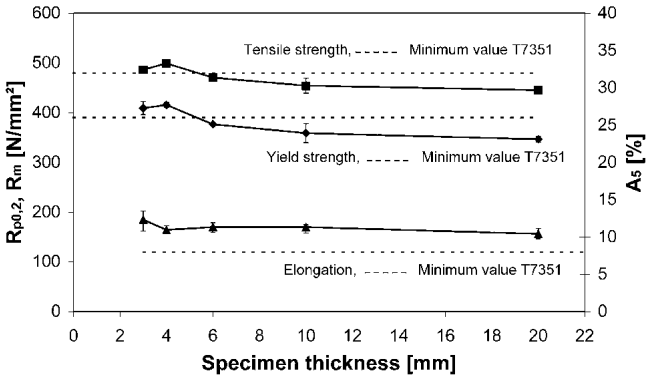

Fig. 7 Strength properties with increasing specimen thickness. Dotted line = minimum values (alloy AW-7075-T7, gas quench 16 bar aged at 120 °C for 12 h + 180 °C for 11 h)

Table 4 Calculated quench factor *Q*, predicted yield strength σ_Y, and measured yield strength after high-pressure gas quenching

AW-7075-T73; σ_{max} = 450 MPa

	Specimen thickness			
Variable	**3 mm**	**6 mm**	**10 mm**	**20 mm**
Quench factor *Q*	4.91	9.00	14.43	31.29
Predicted yield strength (σ_Y), MPa	439	430	418	384
Measured yield strength ($R_{p0.2}$), MPa	409	377	359	347

come if continuous cooling transformation (CCT) diagrams of Al alloys instead of isothermal transformation diagrams existed.[14]

For casting alloy A357.0, it was possible to measure an average cooling rate up to 90 K/s in the temperature interval between 425 and 150 °C. The tensile properties after water and gas quenching are compared in Fig. 9. The minimum requirements for investment castings[15] could be exceeded for water quenching as well as for gas quenching, but it has to be mentioned that the usual aging time of 4 h is not sufficient after gas quenching to obtain the desired tensile properties. The strength

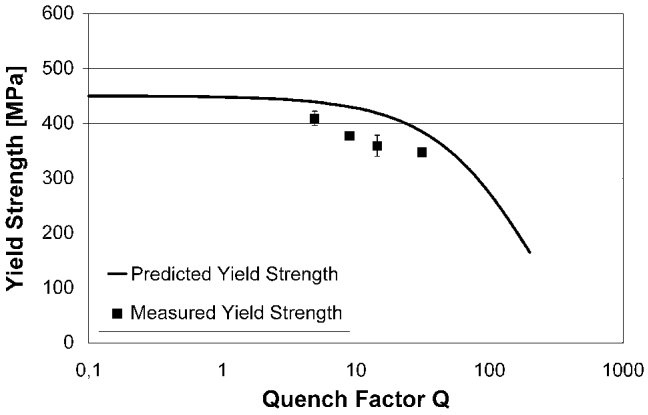

Fig. 8 Predicted and measured yield strength as a function of the quench factor *Q* (alloy 7075-T73)

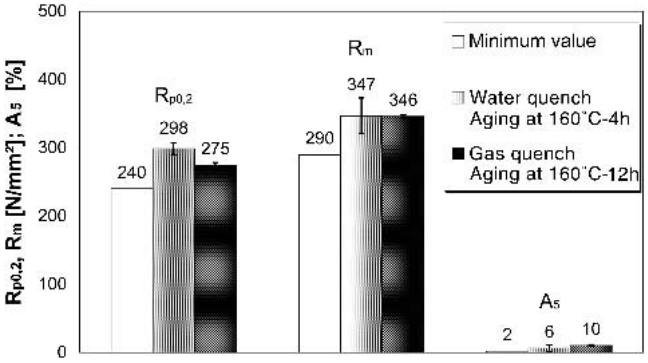

Fig. 9 Strength properties of alloy A357.0-T6 by comparison (Ø8 mm, after gas quenching 16 bar He + aging 160 °C 12 h and after water quenching + aging 160 °C 4 h

properties after gas quenching are further increased with an extended aging time of 12 h at 160 °C. After 12 h, it was possible to achieve a yield strength of 275 MPa and an ultimate tensile strength of 346 MPa with an elongation of 10%.

Vickers hardness measurements have revealed a maximum in hardness after water quenching and aging for approximately 6 h (Fig. 10). After gas quenching, the maximum was found to be at a slightly lower hardness level after an aging time of 10-12 h. One reason for the increasing aging time could be the lower vacancy density after gas quenching necessary for the diffusion of alloying atoms and the creation of precipitates. In the case of a lower vacancy density, the diffusion rate of alloying atoms would decrease and the aging time would increase.[16]

4.2 Nozzle Field Quenching

The cooling curves for the nozzle field quenching have been similarly determined and are plotted in Fig. 11. The cooling rates were again calculated in a temperature interval between 425 and 150 °C. For the thinnest cross section of Ø5 mm, an average cooling rate of 65 K/s was determined (Ø8 mm = 45 K/s; Ø12 mm = 30 K/s).

The tensile properties of AW-2024-T4 after nozzle field

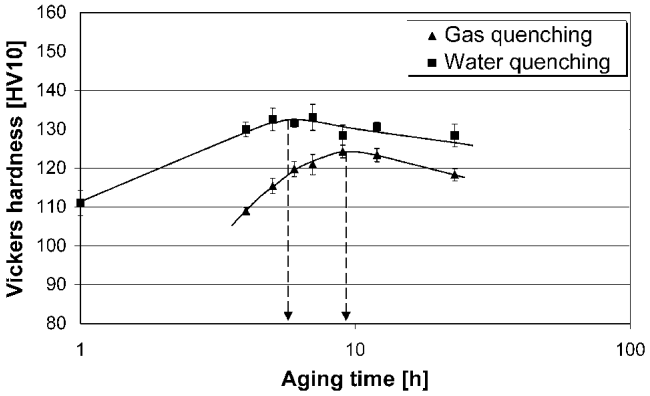

Fig. 10 Aging behavior of alloy A357.0 at 160 °C after water quenching and after gas quenching

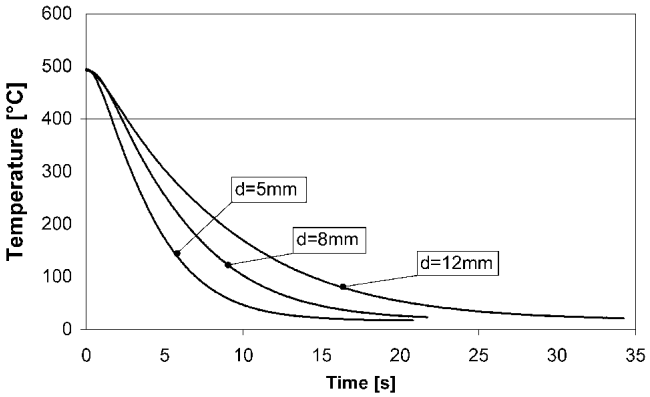

Fig. 11 Cooling curves with different specimen diameters (nozzle field quenching with nitrogen; alloy AW-2024)

quenching and aging are shown in Fig. 12. The mechanical properties exceed the minimum required values[12] for the alloy not only at a diameter of 5 mm, but also at a specimen diameter of 12 mm with a cooling rate of 30 K/s. This equals approximately the cooling rate obtained after high-pressure gas quenching of 2024 (6 mm), leading to comparable mechanical properties.

5. Prospects

The following question arises: which parts of aluminum alloys can use the high-pressure gas quenching or the nozzle field quenching during precipitation hardening? Differences in manufacturing routing have to be considered. In contrast to steels, the machining of aluminum alloys is easily performed in a condition of maximum strength. Thus, parts can be machined after the heat treatment. Because the distortion will be removed by further machining operations, any distortion of the semifinished material plays a minor role. Therefore, high-pressure gas quenching or nozzle field quenching is only economically viable for certain semifinished products.

Castings and forgings are usually in a near-net-shape condition prior to heat treatment. Ideally, only functional surfaces

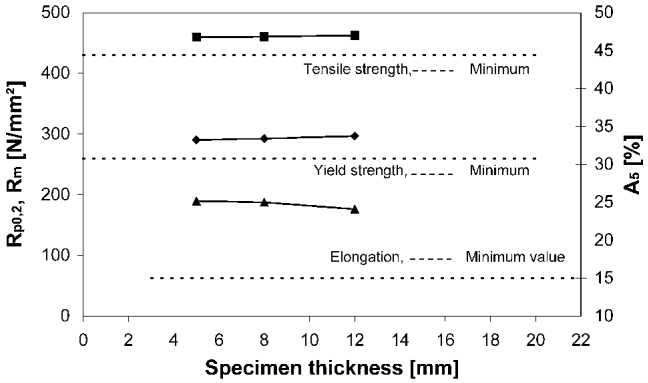

Fig. 12 Strength properties of alloy AW-2024-T4 by comparison (nozzle field quenching; aged at RT for >96 h)

should be machined after the heat treatment. The distortion of castings and forgings often exceeds the form tolerance and requires time- and cost-intensive reworking. High-pressure gas quenching and nozzle field quenching could be interesting alternatives to water quenching in these manufacturing routes, if the desired mechanical properties could be achieved.

It is a common practice to reduce distortion by quenching in hot water or by adding polymers.[1,2,17] This is associated with a reduction in cooling rate and therefore with a loss in strength. To determine the equivalent water temperature that corresponds to the high-pressure gas quenching, a comparison of the cooling rates during gas quenching with helium at 16 bar and water quenching at different water temperatures is represented in Fig. 13.[18] With increasing specimen thickness, the cooling rates decrease. Apart from the cooling rates in water and glycol, the diagram was supplemented by the cooling rates during high-pressure gas quenching with helium at 16 bar for different specimen thicknesses. For all gas-quenched specimens, the cooling rates are situated above that of 40% glycol with a temperature of 21 °C. For the thinnest examined specimen (3.2 mm), the cooling rate corresponded to an equivalent water temperature of 60 °C. Therefore, high-pressure gas quenching as well as nozzle field quenching would be alternatives to quenching in water at higher temperatures or in polymer solutions with relatively high polymer concentrations. It is a fact that quenching in a gaseous medium reduces residual stresses and distortion. Several investigations have demonstrated this for the martensitic hardening of steels.[19-21] The gas quenching of aluminum alloys offers, also, the opportunity for a reduction of residual stresses and distortion during age hardening, because the critical mechanisms for the development of distortion are the same. This will be examined in further investigations.

6. Summary

While maintaining the conventional heat-treating parameters, the precipitation-hardenable aluminum wrought alloys 2024, 6013, and 7075, and the casting alloy A357.0 were quenched in helium at 16 bar instead of water. In the temperature range between 425 and 150 °C, quenching rates of up to 90 K/s could be achieved. The determination of the mechanical

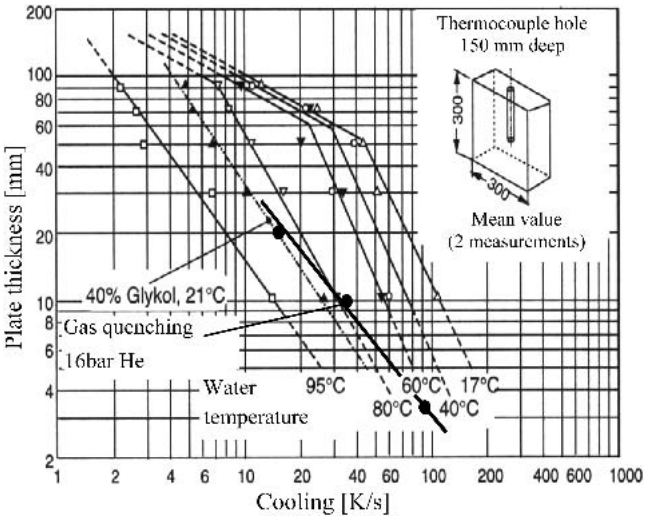

Fig. 13 Cooling rates in water, glycol, and helium (16 bar) in a temperature range between 400 and 290 °C, depending on material thickness. Water and glycol quenching values are from Ostermann.[18]

properties for the examined alloys resulted in sufficient strength after gas quenching and aging up to a thickness of several millimeters compared with the required minimum values. For thin sheets (i.e., 3 mm), nearly similar mechanical properties could be achieved after gas quenching and aging as those after water quenching and aging. In the case of the casting alloy A357.0, a different aging behavior after gas quenching was observed. It was found that the maximum hardness and strength are shifted to slightly lower levels at longer aging times. The tensile strength after the gas nozzle field quenching and aging of alloy 2024 with a specimen diameter between 5 and 12 mm, approximately equals the mechanical properties after high-pressure gas quenching of alloy 2024 (diameter 6 mm) specimens.

Aluminum castings and forgings can be classified as an interesting field for the application of high-pressure gas quenching, or nozzle field quenching, during precipitation hardening. Cost savings would be possible in these manufacturing chains due to reduced distortion and, therefore, to reduced reworking of the parts. A further advantage is the avoidance of intensive cleaning operations of polymer-quenched parts.

Acknowledgments

The authors thank the Bremer Invovations Agentur (BIA) and the Senator fuer Wirtschaft und Haefen, Bremen, Germany for the financial support (AMST P1), as well as Airbus, Bremen, Germany and TITAL, Bestwig, Germany for the test materials provided.

References

1. G.E. Totten, G.M. Webster, and C.E. Bates, An Overview of Aluminum Quenching With Polymer Quenchants, *Ind. Heat.,* Vol 65 (No. 11), 1974, p 61-66
2. C. Ikei, E. Hollis, A. Furman, D. Clark, J. Chavez, P. Huk, R. Tilak, E.W. Lee, and O.S. Es-Said, The Effect of Processing Parameters on the Mechanical Properties and Distortion Behavior of 6061 and 7075 Aluminum Alloy Extrusions, *Mater. Sci. Forum,* Vol 331-337, 2000, p 663-668
3. F.T. Hoffmann, T. Lübben, and P. Mayr, Innovations in Quenching Systems and Equipment: Current Status and Future Developments, *Heat Treat. Met.,* Vol 26 (No. 3), 1999, p 63-67
4. J. Wünning, Single-Part Quenching of Serial Parts with Gas Jets Located in a Mold, Einzelteilhärtung von Serienbauteilen in Gasdüsenformen, *Härt.-Tech. Mitt.,* Vol 48 (No. 3), 1993, p 199-204
5. J.W. Evancho and J.T. Staley, Kinetics of Precipitation in Aluminum Alloys During Continuous Cooling, *Metall. Trans.,* Vol 5, 1974, p 43-47
6. *Heat Treating,* Vol 4, 9th ed., *Metals Handbook*, American Society for Metals, 1981, p 690-691
7. C.E. Bates, Selecting Quenchants to Maximize Tensile Properties and Minimize Distortion in Aluminum Parts, *J. Heat Treat.,* Vol 5 (No. 1), 1987, p 27-40
8. C. Kammer, *Aluminum-Taschenbuch Band 1,* Aluminum-Verlag Düsseldorf, 1998, Vol 1 p 250 (in German)
9. J.R. Davis, Ed., *ASM Specialty Handbook: Aluminum and Aluminum Alloys,* American Society for Metals, 1981, p 71-73
10. B. Edenhofer, An Overview of Advances in Atmosphere and Vacuum Heat Treatment, *Heat Treat. Met.,* Vol 26 (No. 1), 1999, p 1-5
11. Mechanical Properties-6013-T6 Sheet, SPD-10-009, Alloy 6013 Sheet, ALCOA, www.millproducts-alcoa.com/productsandalloys/alloy6013techsheet.pdf, September 2004 (2001)
12. German Institute for Standardization, Materials Handbook of German Aviation, Vol 2 (No. 1) *Werkstoff-Handbuch der Deutschen Luftfahrt, Teil 1, Bd 2,* Deutsches Institut für Normung, Beuth-Verlag GmbH, 1964 (in German)
13. R.R. Sawtell and J.T. Staley, Interactions Between Quenching and Aging in Alloy 7075, *Aluminum,* Vol 59 (No. 2), 1983, p 127-133
14. T. Herding, O. Kessler, F. Hoffmann, and P. Mayr, An Approach for Continuous Cooling Transformation (CCT) Diagrams of Aluminum Alloys, *Mater. Sci. Forum,* Vol 396-402, 2002, p 869-874
15. Aluminum and Aluminum Alloys-Castings-Chemical Composition and Mechanical Properties "Aluminum und Aluminumlegierungen-Gussstücke-Chemische Zusammensetzung und mechanische Eigenschaften," DIN EN 1706, Ausgabe: 1998-06, Beuth Verlag GmbH, 1997 (in German)
16. D.S. MacKenzie, Metallurgical Principles of Quenching Aluminum Alloys, *Proceedings of the 16th ASM Heat Treating Society Conference & Exposition,* 19-21 March 1996 (Cincinnati, OH), ASM International, 1996, p 213-219
17. H. Beitz, Heat Treatment of AGe Hardenable Aluminium Alloys—Preferably Without Distortion, *Werkstoff-Seminare,* München, 1991, p 181-196
18. F. Ostermann, Application Technology Aluminum, *Anwendungstechnologie Aluminum,* Springer-Verlag, 1998, p 64 (in German)
19. O. Kessler, F. Hoffmann, and P. Mayr, Distortion of the Uncoated and CVD Coated Tool Steel D2 After Gas Quenching, Maß-und Formänderungen bei der Gasabschreckung des unbeschichteten und CVD-beschichteten X155CrVMo12-1, *Härt.-Tech. Mitt.,* Vol 50 (No. 6), 1995, p 337-343
20. S. Segerberg and E. Troell, High-Pressure Gas Quenching Using a Cold Chamber to Increase Cooling Capacity, *Heat Treat. Met.,* Vol 24 (No. 1), 1997, p 21-24
21. F. Preißer, K. Löser, S. Segerberg, and E. Troell, High-Pressure Gas Quenching of Case Hardened Steels and Tempered Steels in Cold Chambers, Hochdruck-Gasabschrecken von Einsatz-und Vergütungsstählen in kalten Kammern, *Härt.-Tech. Mitt.,* Vol 52 (No. 5), 1997, p 264-269